Rate of steady-state reconnection in an incompressible plasma

Cite as: Physics of Plasmas **8**, 4800 (2001); https://doi.org/10.1063/1.1410112
Submitted: 13 July 2000 . Accepted: 09 July 2001 . Published Online: 19 October 2001

Nikolai V. Erkaev, Vladimir S. Semenov, Ilya V. Alexeev, and Helfried K. Biernat

Rate of steady-state reconnection in an incompressible plasma

Nikolai V. Erkaev
Institute of Computational Modelling, Russian Academy of Sciences, 660036 Krasnoyarsk 36, Russia

Vladimir S. Semenov and Ilya V. Alexeev
Institute of Physics, University of St. Petersburg, St. Petergof 198504, Russia

Helfried K. Biernat[a)]
Space Research Institute, Austrian Academy of Sciences, Schmiedlstrasse 6, A-8042 Graz, Austria

(Received 13 July 2000; accepted 9 July 2001)

The reconnection rate is obtained for the simplest case of two-dimensional (2D) symmetric reconnection in an incompressible plasma. In the short note [Erkaev *et al.*, Phys. Rev. Lett. **84**, 1455 (2000)], the reconnection rate is found by matching the outer Petschek solution and the inner diffusion region solution. Here the details of the numerical simulation of the diffusion region are presented and the asymptotic procedure which is used for deriving the reconnection rate is described. The reconnection rate is obtained as a decreasing function of the diffusion region length. For a sufficiently large diffusion region scale, the reconnection rate becomes close to that obtained in the Sweet–Parker solution with the inverse square root dependence on the magnetic Reynolds number Re_m, determined for the global size of the current sheet. On the other hand, for a small diffusion region length scale, the reconnection rate turns out to be very similar to that obtained in the Petschek model with a logarithmic dependence on the magnetic Reynolds number Re_m. This means that the Petschek regime seems to be possible only in the case of a strongly localized conductivity corresponding to a small scale of the diffusion region. © *2001 American Institute of Physics.* [DOI: 10.1063/1.1410112]

I. INTRODUCTION

Magnetic reconnection is a physical process in plasmas which changes magnetic-field topology and releases stored magnetic energy. It is one of the central concerns in astrophysical, solar, space, fusion and laboratory plasmas (e.g., Hones;[1] Priest[2]).

A key question arising in the reconnection theory is that of the reconnection rate. So far there are two different magnetohydrodynamic (MHD) models of reconnection based on the Sweet–Parker (pure diffusion) (see Parker;[3] Sweet[4]) and the Petschek (slow shock energy conversion) (see Petschek[5]) approaches. These models propose two different estimations of the reconnection rate ε: The Sweet–Parker model predicts $\varepsilon \sim 1/\sqrt{Re_m}$, and the Petschek model gives $\varepsilon \sim 1/\ln Re_m$, where

$$Re_m = \frac{4\pi V_A L}{c^2 \eta}, \tag{1}$$

is the global magnetic Reynolds number based on the half-length of a current layer L, the Alfvén velocity V_A, and the resistivity of the plasma η. For cosmic plasmas, magnetic Reynolds numbers usually are very large, therefore, the Petschek regime seems to be much more effective. However, since the Petschek reconnection model was proposed, it is not clear what conditions are necessary to realize this regime.

It is a fact that numerical simulations (Biskamp;[6] Scholer[7]) carried out for a constant resistivity were not able to reproduce the solution of Petschek type, instead, they were rather in favor of the Sweet–Parker solution. Laboratory experiments also seem to observe the Sweet–Parker regime of reconnection (Ji *et al.*[8]).

On the other hand, if nonuniform resistivity is localized to a small region, the results of numerical simulations (Scholer;[7] Ugai[9]) clearly show Petschek-type reconnection with pronounced slow shocks. For the Petschek regime, there are two physically different regions: A small diffusion region, where dissipation is important, is surrounded by a large convective zone where the plasma can be considered as ideal and dissipationless. The problem is very complicated and thus it does not seem realistic to obtain an analytical solution which is valid for both regions simultaneously. To simplify this problem, we seek solutions separately, in the diffusion region and in the convective zone. For the latter, a solution can be obtained analytically as an asymptotic series with respect to a small reconnection rate. For the diffusion region, it is impossible to find an analytical solution, and hence it has to be obtained numerically. In this semianalytical approach, we have to combine the numerical solution for the diffusion region and the Petschek analytical solution for the convective region. The latter can be done by different methods, which lead to absolutely identical results for the reconnection rate estimation. The estimation obtained by Erkaev *et al.*[10] is based on asymptotic matching of the diffusion region and convective zone solutions. In our present work, we use another way based on a regularized convective region solution, which seems to be rather clear and very close to the original Petschek method. In this paper we give a detailed description of the numerical solution for the diffusion region,

a)Electronic mail: helfried.biernat@kfunigraz.ac.at

and derive the estimation for the reconnection rate.

This paper is organized as follows: In Secs. II and III, we start with the steady-state MHD equations and present the Petschek solution. The diffusion region scaling and boundary layer equations are introduced in Sec. IV. The numerical algorithm and the results of the calculations are described in Secs. V and VI. The reconnection rate is derived in Sec. VII, whereas Sec. VIII is devoted to the summary and discussion. Mathematical details are described in the Appendix.

II. MHD EQUATIONS

In the problem under consideration, the plasma is governed by the resistive steady-state MHD system of equations

$$\rho(\mathbf{v}\cdot\nabla)\mathbf{v}=-\nabla\mathbf{P}+\frac{\mathbf{1}}{\mathbf{4}\pi}(\mathbf{B}\cdot\nabla)\mathbf{B}, \tag{2}$$

$$\mathbf{E}+\frac{1}{c}(\mathbf{v}\times\mathbf{B})=\frac{c}{4\pi}\eta(x,y)\,\mathrm{curl}\,\mathbf{B}, \tag{3}$$

$$\nabla\cdot\mathbf{B}=0,\quad \nabla\cdot\mathbf{v}=0, \tag{4}$$

where ρ is a mass density, P is the total pressure, $P=p+B^2/8\pi$, and Re_m is the global magnetic Reynolds number based on the maximal value of the resistivity $\eta_{\max}$.

Outside of the diffusion region, in the so-called convection zone, dissipation is not important any longer, and we can use the ideal system of MHD equations in the limit $Re_m\to\infty$.

In an incompressible plasma the following relations have to be satisfied at the shock front:

$$\{B_n\}=0, \tag{5}$$

$$\{v_n\}=0, \tag{6}$$

$$\{P\}=0, \tag{7}$$

$$\left\{\frac{1}{4\pi}B_n\mathbf{B}_t-\rho v_n\mathbf{v}_t\right\}=0, \tag{8}$$

$$\{B_n\mathbf{v}_t-v_n\mathbf{B}_t\}=0, \tag{9}$$

where the subscripts n and t denote components normal and tangential to the shock front.

III. PETSCHEK SOLUTION

The Petschek solution, which is valid in the convection region, can be presented as follows (Petschek,[5] for details see Vasyliunas[11]). We use coordinates x, y, which are directed along the current sheet and in the perpendicular direction, respectively. The solution is completely determined by the following parameters: Quantity L which is the halflength of the current sheet, v_0 is the plasma inflow velocity, and B_0 is the initial magnetic field. The solution is presented in the form of asymptotic series with respect to the small parameter which is known as the reconnection rate

$$\varepsilon=\frac{v_0}{V_A}=\frac{E_0}{E_A}\ll 1. \tag{10}$$

Here E_0 is the electric field which is constant in the 2D case under consideration, and $E_A=(1/c)V_AB_0$ is the Alfvén electric field.

Inflow region

$$v_x=0,\quad v_y=-\varepsilon V_A, \tag{11}$$

$$B_x=B_0-\frac{4\varepsilon B_0}{\pi}\ln\frac{L}{\sqrt{x^2+y^2}},\quad B_y=\frac{4\varepsilon B_0}{\pi}\arctan\frac{x}{y}. \tag{12}$$

Outflow region

$$v_x=V_A,\quad v_y=0, \tag{13}$$

$$B_x=0,\quad B_y=\varepsilon B_0. \tag{14}$$

The equation for the shock in the first quadrant is

$$y=\varepsilon x. \tag{15}$$

It can be shown that slightly outside of the shock from the inflow side

$$B_y(x,0)=\begin{cases}2\varepsilon B_0x & >0\\ -2\varepsilon B_0x & <0\end{cases}. \tag{16}$$

Expressions (11)–(16) are asymptotic solutions with respect to ε (zero- and first-order terms in the inflow region and only zero-order term in the outflow region) of the ideal MHD system of Eqs. (2)–(4) and the Rankine–Hugoniot shock relations (5)–(9).

Petschek did not obtain a solution in the diffusion region, instead, he estimated the maximum reconnection rate as $1/\ln Re_m$ using some simple physical suggestions. Generally speaking, this implies that the Petschek model gives any reconnection rate from the Sweet–Parker value $1/\sqrt{Re_m}$ up to $1/\ln Re_m$, and for a long time, it was unclear whether Petschek reconnection faster than Sweet–Parker reconnection is possible. This problem can be solved by combining the analytical Petschek solutions (11)–(16) and the numerical model of the diffusion region.

IV. DIFFUSION REGION SCALING

The next step is to find a numerical solution for the diffusion region. But first we have to obtain the boundary layer MHD equations suitable for the diffusion region.

To this end we renormalize the MHD equations to new scales B_d, V_{Ad}, $E_{Ad}=B_dV_{Ad}/c$, P_d, where all quantities are supposed to be taken at the upper boundary of the diffusion region

$$x'=x/l_\eta,\quad y'=y/l_\eta,\quad \mathbf{B}'=\mathbf{B}/B_d,\quad \mathbf{v}'=\mathbf{v}/V_{Ad},\quad P'=P/P_d, \tag{17}$$

where l_η is the characteristic length of the resistivity variation. The diffusion region length scale l_d (see Fig. 1) obtained from our numerical results (Sec. VII) is of order of the scale l_η.

The convective electric field $-\mathbf{v}\times\mathbf{B}/c$ is zero in the center of the diffusion region $x=y=0$ where $\mathbf{v}=\mathbf{B}=0$, and then increases to the constant value E_0 at the boundary of the convection zone. This type of behavior of the convective electric field is reasonable to be used for the definition of the

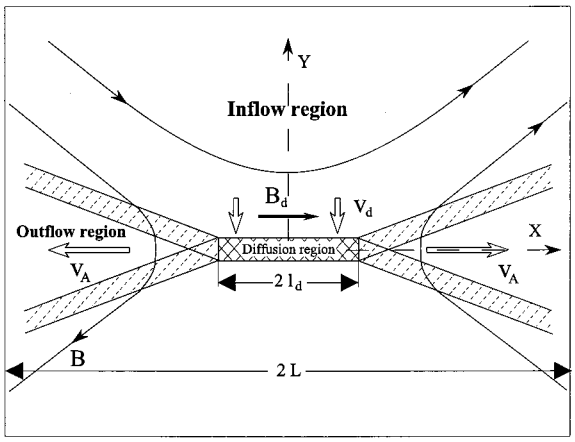

FIG. 1. Scheme of Petschek reconnection.

size of the diffusion region which is one of the most important parameters of the problem. Namely, the length scale of the diffusion region is determined as the distance between the origin $x=0$, $y=0$ and the boundary where the convective electric field reaches its asymptotic value E_0, or better to say, some level, for example, $0.9E_0$.

In the diffusion region where dissipation is essential, we adopt the dissipative MHD equations with the magnetic Reynolds number

$$Re'_d=\frac{4\pi V_{Ad} l_\eta}{c^2 \eta_{\max}}, \tag{18}$$

and the normalized electric field $E'=Ec/(V_{Ad}B_d)=\varepsilon'$, where ε' is a local reconnection rate at the diffusion region boundary. The electric field and local reconnection rate are not known. They are to be obtained from the numerical solution for the diffusion region.

The scaling for the diffusion region is similar to that for the Prandtl viscous layer (Landau and Lifschitz[12]) and corresponds exactly to the Sweet–Parker one

$$x',B'_x,v'_x,P'\sim O(1), \quad y',B'_y,v'_y,\varepsilon'\sim 1/\sqrt{Re'_d}. \tag{19}$$

Consequently, the new boundary layer variables are as follows:

$$\begin{aligned}&\tilde{x}=x', \quad \tilde{B}_x=B'_x, \quad \tilde{v}_x=v'_x, \quad \tilde{P}=P', \quad \tilde{y}=y'\sqrt{Re'_d},\\ &\tilde{B}_y=B'_y\sqrt{Re'_d}, \quad \tilde{v}_y=v'_y\sqrt{Re'_d}, \quad \tilde{\varepsilon}=\varepsilon'\sqrt{Re'_d}.\end{aligned} \tag{20}$$

The diffusion region Reynolds number Re'_d is certainly smaller then the global Reynolds number Re_m, but still it is supposed to be $Re'_d \gg 1$. Therefore, in zero-order with respect to $1/Re'_d$, the boundary layer equations turn out to be

$$\frac{\partial \tilde{v}_x}{\partial t}+\tilde{v}_x\frac{\partial \tilde{v}_x}{\partial \tilde{x}}+\tilde{v}_y\frac{\partial \tilde{v}_x}{\partial \tilde{y}}-\tilde{B}_x\frac{\partial \tilde{B}_x}{\partial \tilde{x}}-\tilde{B}_y\frac{\partial \tilde{B}_x}{\partial \tilde{y}}=-\frac{\partial \tilde{P}}{\partial \tilde{x}}, \tag{21}$$

$$\frac{\partial \tilde{P}}{\partial \tilde{y}}=0, \tag{22}$$

$$\frac{\partial \tilde{B}_x}{\partial t}=\frac{\partial}{\partial \tilde{y}}(\tilde{v}_x\tilde{B}_y-\tilde{v}_y\tilde{B}_x)+\frac{\partial}{\partial \tilde{y}}\left(\tilde{\eta}(\tilde{x},\tilde{y})\frac{\partial \tilde{B}_x}{\partial \tilde{y}}\right)-\mu\frac{\partial}{\partial \tilde{y}}\left(\tilde{\eta}(\tilde{x},\tilde{y})\frac{\partial \tilde{B}_y}{\partial \tilde{x}}\right), \tag{23}$$

$$\frac{\partial \tilde{B}_y}{\partial t}=-\frac{\partial}{\partial \tilde{x}}(\tilde{v}_x\tilde{B}_y-\tilde{v}_y\tilde{B}_x)-\frac{\partial}{\partial \tilde{x}}\left(\tilde{\eta}(\tilde{x},\tilde{y})\frac{\partial \tilde{B}_x}{\partial \tilde{y}}\right)+\mu\frac{\partial}{\partial \tilde{x}}\left(\tilde{\eta}(\tilde{x},\tilde{y})\frac{\partial \tilde{B}_y}{\partial \tilde{x}}\right), \tag{24}$$

$$\frac{\partial \tilde{B}_x}{\partial \tilde{x}}+\frac{\partial \tilde{B}_y}{\partial \tilde{y}}=0, \tag{25}$$

$$\frac{\partial \tilde{v}_x}{\partial \tilde{x}}+\frac{\partial \tilde{v}_y}{\partial \tilde{y}}=0, \tag{26}$$

where $\tilde{\eta}(\tilde{x},\tilde{y})$ is the normalized resistivity of the plasma with the maximum value to be 1, μ is a small parameter, $\mu=1/Re'_d$. The small terms which include μ at the right sides of the induction equations are necessary for numerical stability of the calculations.

It can be seen from Eq. (22) that the total pressure is constant across the diffusion region. This is a general feature of a boundary layer approximation. Hence, the total pressure is defined inside the diffusion region by values at the boundary, and for the boundary layer equations (21)–(26), the total pressure can be considered to be a given function of x, e.g., $\tilde{P}(\tilde{x})$.

As it was pointed out, the appropriate exact solutions of the boundary layer equations (21)–(26) are unknown even in the steady-state case, therefore, we have to solve the problem numerically. Although we have to obtain a steady-state solution, from the point of view of simulation, it is advantageous to use a relaxation method and to solve numerically the unsteady system of the boundary layer MHD equations (21)–(26).

It is important to note that in the subset of Eqs. (23)–(25), only two equations are independent. In principle, we can determine the normal component from the induction equation (24) or from Eq. (25) providing the magnetic flux conservation. From the mathematical point of view, they are equivalent. In our numerical solution, we use Eq. (25) to determine the $\tilde{B}_y$ component in the internal grid points, and Eq. (24) is used as a boundary condition at the lower boundary.

V. NUMERICAL ALGORITHM

Starting with an initial MHD configuration under fixed boundary conditions, we look for the convergence of the time-dependent solution to a steady state. To avoid additional numerical diffusion, we do not use a flux function and a magnetic potential. The normalized total pressure is chosen to be 1.

The distribution of the resistivity $\eta=\eta_{\max}\tilde{\eta}(x,y)$ is traditional (Scholer;[7] Ugai[9])

$$\tilde{\eta}(\tilde{x},\tilde{y}) = de^{(-s_x\tilde{x}^2 - s_y\tilde{y}^2)} + f, \tag{27}$$

with $d+f=1$. Setting $d=0.95$ and $f=0.05$ we can model a case of localized resistivity, for $d=0$ and $f=1$ the resistivity is uniform.

As the initial configuration, we choose a current sheet with a linear profile of the magnetic-field $\tilde{B}_x=\tilde{y}$, $\tilde{B}_y=0$. The velocity components are assumed to be equal to zero at the initial moment, $\tilde{V}_x=0$, $\tilde{V}_y=0$.

To solve the MHD system numerically, we use a two step conservative finite difference numerical scheme with a rectangular grid 145×100 in the first quadrant. From a time level (n), we calculate the parameters on the next time level $(n+1)$ in two steps. In the first step $(n+1/2)$, diffusion is switched off, and we calculate the parameter at the intermediate points $(n+1/2)$ using the equations in characteristic form. This is similar to the approach used in the Godunov method. In the second step, we calculate the parameters at the next time level $(n+1)$ using the equations in conservative form and taking into account the diffusion terms approximated in implicit form.

The details of the numerical algorithm are the following. The $\tilde{B}_x$ component is found from the x-component of the induction equation

$$[(B_x)^{n+1}_{i,k}-(B_x)^{n}_{i,k}]/\tau+(G^{n+1/2}_{i,k+1/2}-G^{n+1/2}_{i,k-1/2})/hx = \left[\frac{\partial}{\partial\tilde{y}}\left(\eta(\tilde{x},\tilde{y})\frac{\partial\tilde{B}_x}{\partial\tilde{y}}\right)\right]^{n+1}_{i,k} - \mu\left[\frac{\partial}{\partial\tilde{y}}\left(\eta(\tilde{x},\tilde{y})\frac{\partial\tilde{B}_y}{\partial\tilde{x}}\right)\right]^{n+1}_{i,k}, \tag{28}$$

where the parameters

$$G^{n+1/2}_{i,k+1/2}=(\tilde{B}_x\tilde{V}_y-\tilde{V}_x\tilde{B}_y)^{n+1/2}_{i,k+1/2}, \tag{29}$$

are determined by the method of characteristics on the level $n+1/2$. This implies that at the beginning $(n\to n+1/2)$ diffusion is switched off, and only convection acts, and then for given convection, diffusion is switched on, and $\tilde{B}_x$ is calculated on the level n. The normal magnetic-field component $\tilde{B}_y$ is determined from the equation $\nabla\cdot\mathbf{B}=0$.

The velocity component $\tilde{V}_x$ is found from the x-component of the momentum equation (21)

$$[(\tilde{V}_x)^{n+1}_{i,k}-(\tilde{V}_x)^{n}_{i,k}]/\tau+(Q_{yi,k+1/2}-Q_{yi,k-1/2})^{n+1/2}/hy + (Q_{xi+1/2,k}-Q_{yi-1/2,k})^{n+1/2}/hx=0, \tag{30}$$

where

$$Q^{n+1/2}_{yi,k+1/2}=(\tilde{V}_x\tilde{V}_y-\tilde{B}_x\tilde{B}_y)^{n+1/2}_{i,k+1/2}, \tag{31}$$

$$Q^{n+1/2}_{xi+1/2,k}=(V_x^2-B_x^2)^{n+1/2}_{i+1/2,k}. \tag{32}$$

Here, the parameters $()^{n+1/2}_{i,k+1/2}$ are determined by the method of characteristics on the level $n+1/2$ simultaneously with the calculation of $\tilde{B}_x$. The velocity component $\tilde{V}_y$ is determined from the equation $\mathrm{div}\,\mathbf{V}=0$.

The boundary conditions are as follows:

At the upper (inflow) boundary, the tangential magnetic-field component is assumed to be constant, $\tilde{B}_x=1$ and the tangential velocity component vanishes $\tilde{V}_x=0$.

At the left boundary we have the symmetry conditions, $\partial\tilde{B}_x/\partial\tilde{x}=0$, $\tilde{B}_y=0$, $\tilde{V}_x=0$.

At the right boundary we hold free conditions suitable for a uniform flow in the outflow region, $\partial\tilde{B}_y/\partial\tilde{x}=0$, $\partial\tilde{V}_y/\partial\tilde{x}=0$.

At the lower boundary $(y=0)$ there is the symmetry condition for the tangential magnetic-field component, $\tilde{B}_x=0$, and the nonflow condition for the normal velocity component, $\tilde{V}_y=0$. At this boundary, the normal component of the magnetic-field $\tilde{B}_y$ is obtained from the induction equation (24) on the line $y=0$

$$\frac{\partial\tilde{B}_y}{\partial t}+\frac{\partial}{\partial t}(\tilde{V}_x\tilde{B}_y)=-\frac{\partial}{\partial\tilde{x}}\left(\eta(\tilde{x},\tilde{y})\frac{\partial\tilde{B}_x}{\partial\tilde{y}}\right) + \mu\frac{\partial}{\partial\tilde{x}}\left(\eta(\tilde{x},\tilde{y})\frac{\partial\tilde{B}_y}{\partial\tilde{x}}\right). \tag{33}$$

The small parameter $\mu\sim0.1-0.2$ is used here to regularize the numerical scheme for the unsteady system of the boundary layer MHD equations (21)–(26), which is an ill-posed problem in our case.

The size of the computational domain is chosen to be much larger than the diffusion region size l_d, and also much less than the global size L. At the inflow boundary we do not fix the normal components of the magnetic field and velocity, and thus we do not impose a reconnection rate and an electric field in the diffusion region from the very beginning. The latter has to be found from the numerical solution self-consistently.

VI. RESULTS OF THE NUMERICAL SIMULATION

To estimate the convergence of the time-dependent solution to a steady state for each nth time step, we use the following criteria, $\max(|V^n_x-V^{n-1}_x|)/(\Delta t|V^n_{x\,\max}|)<10^{-6}$. In the 2D steady state the total (convective plus dissipative) electric field must be constant, and it is so in our simulations (see Figs. 2 and 3) besides of small perturbations near the outflow boundary due to some reflections, although we apply free boundary conditions.

Let us discuss the result of our simulations. For the case of localized resistivity, the system reaches the Petschek steady state with clear asymptotic behavior (see Fig. 2): $\tilde{V}_x\to1$ in the outflow region; $\tilde{V}_y\to\tilde{\varepsilon}$ at the inflow boundary; $\tilde{B}_x$ decreases from 1 to 0 at the shock transition; $\tilde{B}_y\to\tilde{\varepsilon}$ in the outflow region; and $\tilde{B}_y\to2\tilde{\varepsilon}$ from the inflow side of the shock [compare with the Petschek solutions (11)–(15)].

There is a well pronounced slow shock, as can be seen in the behavior of all MHD parameters, but in particular in the distribution of the current density. The normalized electric field (reconnection rate) turns out to be $\tilde{\varepsilon}\sim0.7$. It is important to note that the numerical results do not depend on the size of calculation box.

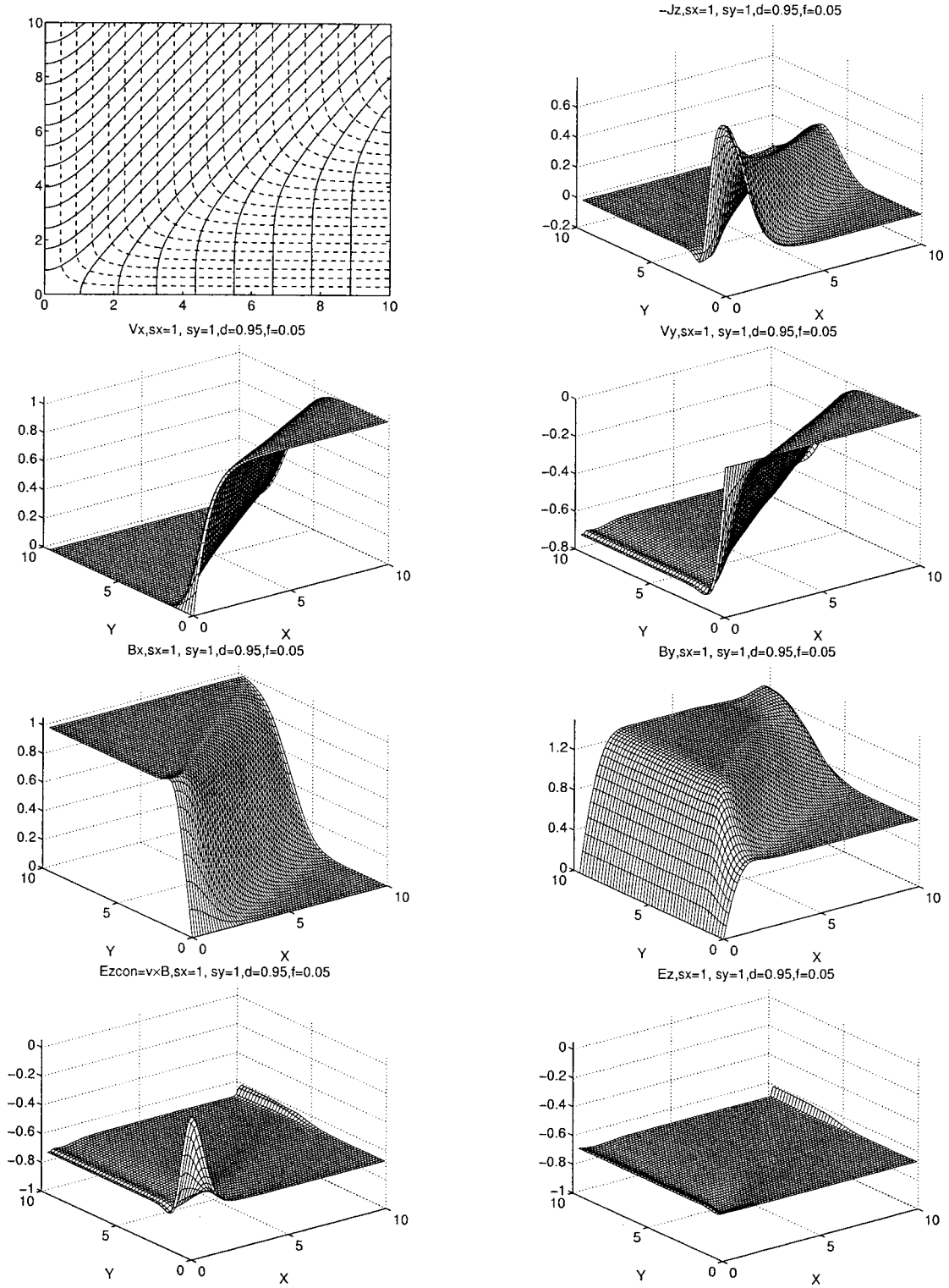

FIG. 2. Numerical results for Petschek-type reconnection with localized resistivity. Left column: Structure of magnetic-field lines (solid lines) and stream lines (dashed), distributions of the V_x, B_x, and convection electric field. Right column: Distributions of the electric current, V_y, B_y, and total electric field.

On the other hand, for the case of homogeneous resistivity, the system reaches the Sweet–Parker state (see Fig. 3), even if the Petschek solution is used as initial configuration (see also Scholer;[7] Ugai;[9] Uzdenski and Kulsrud[13]). This seems to imply that Petschek-type reconnection is possible only if the resistivity of the plasma is localized to a small region, whereas for constant resistivity, the Sweet–Parker regime is realized (Erkaev *et al.*[10]).

The size of the diffusion region layer l_d is defined as its length along the x axis where the convective electric field at the lower boundary $(y=0)$ $\tilde{E}_c=-\tilde{v}_x\tilde{B}_y$ is less in absolute value than some level of the total electric field (say $0.9\tilde{\varepsilon}$).

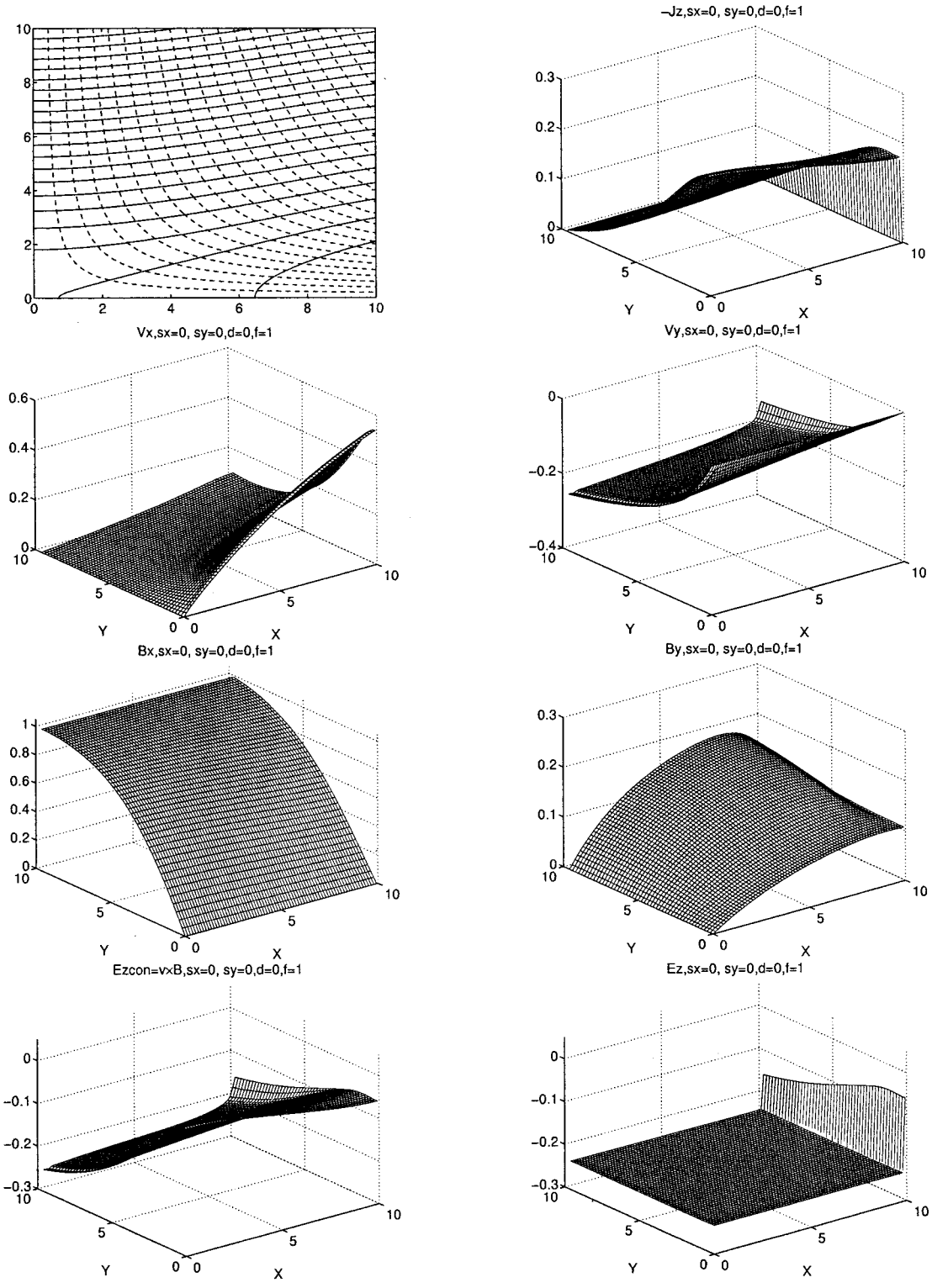

FIG. 3. Numerical results for Sweet–Parker reconnection with constant resistivity. Left column: Structure of magnetic-field lines (solid lines) and stream lines (dashed), distributions of the V_x, B_x, and convection electric field. Right column: Distributions of the electric current, V_y, B_y, and total electric field.

For the case of a localized resistivity, l_d practically coincides with the scale of the inhomogeneity of the resistivity l_η when the maximum of resistivity is much larger then the background resistivity. Therefore, hereafter we consider $l_d \sim l_\eta$.

For the case of uniform resistivity, the plasma is accelerated very slowly, and there is no obvious definition for the scale length of the diffusion region. Diffusion is important everywhere for the pure Sweet–Parker regime, and for the Petschek asymptotic solution there is left no room. Therefore, the solution does not converge to the Petschek solution,

not only at the right-hand boundary but everywhere. In this case, the solution will depend on the calculation box size because it does not have any other scale. Hence, the constant resistivity solution cannot be matched to the Petschek solution.

Nevertheless, the Sweet–Parker regime is still important also for the Petschek solution, because in the nearest vicinity of the reconnection line, where the resistivity can be considered to be constant, the diffusion region structure is similar to the Sweet–Parker case. Besides, and this is even more important, the scaling for the diffusion region is exactly the Sweet–Parker one (19, 20), or, better to say, the Prandtl scaling.

VII. RECONNECTION RATE

To find a relationship between the reconnection rate and dissipation we need first of all an estimation of magnetic field at the boundary of the diffusion region B_d. To this end we cannot use the Petschek solution (12) because the B_x component diverges at the origin $B_x \to -\infty$, when $r=\sqrt{x^2+y^2}\to 0$. This singularity is a consequence of the fact that dissipation actually has not been taken into account for the Petschek solution. Formally it follows from the jump at the origin of the B_y component of the magnetic-field (16). Dissipation evidently leads to smooth behavior of the magnetic field in the diffusion region, and then no singularities are possible. To illustrate this we consider a model distribution of the $B_y(x,0)$ component with linearly smoothed boundary condition at the interval $(-l_d, l_d)$ similar to the original Petschek[5] consideration

$$B_y^P(x,0)=\begin{cases} \pm 2\varepsilon B_0 & L>|x|>l_d \\ 2\varepsilon B_0 \dfrac{x}{l_d} & |x|<l_d \\ 0 & |x|>L \end{cases}. \tag{34}$$

The $B_x(x,y)$ component of the magnetic field in the inflow region can be found from the Poisson integral

$$\begin{aligned} B_x(x,y) &= B_0-\frac{1}{\pi}\int_{-\infty}^{+\infty}\frac{B_y^P(x',0)(x'-x)}{(x'-x)^2+y^2}\,dx' \\ &= B_0-\frac{2\varepsilon B_0}{\pi l_d}\left(2l_d+\frac{x}{2}\ln\frac{(x-l_d)^2+y^2}{(x+l_d)^2+y^2}\right. \\ &\quad \left. + y\arctan\frac{x-l_d}{y}-y\arctan\frac{x+l_d}{y}\right) \\ &\quad -\frac{\varepsilon B_0}{\pi}\left(\ln\frac{(y^2+(L-x)^2)(y^2+(L+x)^2)}{(y^2+(l_d-x)^2)(y^2+(l_d+x)^2)}\right). \end{aligned} \tag{35}$$

This solution does not have a singularity at the origin any more, and tends to the Petschek solution (12) outside the diffusion region. We can simplify Eq. (35) at the origin

$$B_x(0,0)=B_0-\frac{4\varepsilon B_0}{\pi}\ln\frac{L}{l_d}-\frac{4\varepsilon B_0}{\pi}. \tag{36}$$

The first term on the right-hand side of this equation is of the order of $O(1)$, the third one is of $O(\varepsilon)$, but the second term consists of a large parameter $\ln(L/l_d)$ times the small parameter ε. Thus we assume the following relations between the parameters

$$1>\varepsilon\ln\frac{L}{l_d}\gg\varepsilon. \tag{37}$$

So far we considered only a model distribution of the $B_y^P(x,0)$ (34) along the current sheet but it turns out that $B_x(0,0)$ does not depend on the actual distribution of the B_y component inside the diffusion region up to $O(\varepsilon)$. This implies that we can extend Eq. (36) to the general case.

Let us consider the Poisson integral with the actual distribution of the $B_y(x,0)$ component using the model boundary condition $B_y^P(x,0)$ (34) for regularization

$$\begin{aligned} B_x(0,0) &= B_0-\frac{1}{\pi}\int_{-\infty}^{+\infty}\frac{B_y(x',0)}{x'}\,dx' \\ &= B_0-\frac{1}{\pi} \\ &\quad \times\int_{-\infty}^{+\infty}\frac{(B_y(x',0)-B_y^P(x',0)+B_y^P(x',0))}{x'}\,dx' \\ &= B_0-\frac{4\varepsilon B_0}{\pi}\ln\frac{L}{l_d}-\frac{4\varepsilon B_0}{\pi} \\ &\quad +\frac{1}{\pi}\int_{-\infty}^{+\infty}\frac{(B_y(x',0)-B_y^P(x',0))}{x'}\,dx' \\ &= B_0-\frac{4\varepsilon B_0}{\pi}\ln\frac{L}{l_d}-C\varepsilon B_0, \end{aligned} \tag{38}$$

where $C=\text{const}$ includes both, the contribution from $4\varepsilon B_0/\pi$ and the contribution from the nonsingular integral in the fifth line of this equation. The main difficulty for the estimation of this integral is that near the diffusion region, the local Petschek solution reproduced in our simulation, seems to be different from the global one because $\varepsilon'>\varepsilon$ and $B_d<B_0$. The local Petschek solution has asymptotically $B_y(x/l_d)\to 2\varepsilon' B_d$ when $x/l_d\to\infty$ which seems to be different from the condition $B_y^P(x/l_d)\to 2\varepsilon B_0$ used in (34). However, as it is shown in the Appendix, the difference $O(\varepsilon')-O(\varepsilon)$ is of the order of ε rather then $O(\varepsilon\ln(L/l_d))$ (see Appendix). This allows us to estimate the integral (38) as a quantity of order ε which is much smaller than the main term $\sim\varepsilon\ln(L/l_d)$.

The diffusion region is small $l_d\ll L$ and for the boundary condition for the diffusion region B_d we can use the magnetic field at the origin $B_x(0,0)$. Using the relation (38), we find the magnetic-field strength at the diffusion region boundary

$$B_d=B_0\left(1-\frac{4\varepsilon}{\pi}\ln\frac{L}{l_d}\right). \tag{39}$$

Now everything is ready to determine the reconnection rate. The electric field must be constant in the whole inflow region, hence

$$v_d B_d = v_0 B_0, \tag{40}$$

$$\varepsilon' B_d^2 = \varepsilon B_0^2, \tag{41}$$

where the definition of the reconnection rates $\varepsilon' = v_d/B_d$, $\varepsilon = v_0/B_0$ are used. Bearing in mind that $\varepsilon' = \tilde{\varepsilon}/\sqrt{Re}'_d$ [see scaling (20)] we obtain

$$\tilde{\varepsilon} B_d^{3/2} = \varepsilon B_0^{3/2} \sqrt{\frac{4\pi V_{Ad} l_d}{c^2 \eta_{\max}}}. \tag{42}$$

Substituting B_d from Eq. (39), we determine finally the following equation for the reconnection rate ε

$$\tilde{\varepsilon}\left(1 - \frac{4\varepsilon}{\pi} \ln \frac{L}{l_d}\right)^{3/2} = \varepsilon \sqrt{Re_d}, \tag{43}$$

where the magnetic Reynolds number $Re_d = 4\pi V_A l_d/(c^2 \eta_{\max})$ is based on the global Alfvén velocity and the half length of the diffusion region l_d. The internal reconnection rate $\tilde{\varepsilon}$ has to be found from the simulation of the diffusion region problem.

For small $\varepsilon \ln(L/l_d)$ there is an analytical expression

$$\varepsilon = \frac{\tilde{\varepsilon}}{\sqrt{Re_d} + \frac{6}{\pi}\tilde{\varepsilon} \ln \frac{L}{l_d}}. \tag{44}$$

Here $\tilde{\varepsilon}$ is an internal reconnection rate, determined from the numerical solution, which is $\tilde{\varepsilon} \sim 0.7$ for the Petschek type solution.

In the Appendix it is also shown that the global Petschek solution with second-order corrections tends to the asymptotic of the diffusion region solution for $x \sim l_d$.

It is interesting that for the derivation of the final results (43) and (44) the only value which has been actually used is the internal reconnection rate $\tilde{\varepsilon}$ obtained from the numerical solution, and the asymptotic behavior (34). The actual distribution of the B_y component along the upper boundary of the diffusion region does not contribute at all [besides of the asymptotic behavior (34)] in zero-order approximation considered above. Of course, from the mathematical point of view, it is important that the diffusion region solution exists and has the Petschek-type asymptotic behavior (11)–(16). Therefore, the asymptotic behavior (34) plays the key role in the derivation of the reconnection rate and this question needs to be clarified in more detail.

VIII. DISCUSSION

Equations (43) and (44) give the unique reconnection rate for known parameters of the current sheet L, B_0, V_A, η, l_d. Let us fix now the lengths L and start to vary l_d assuming $l_\eta \sim l_d$. It is clear that for small l_d, the Petschek term becomes large, whereas for big l_d, the Sweet–Parker term is dominant. The behavior of the implicit function $\varepsilon(l_d/L)$ given by (43) is nonmonotonic. There exists a length l_d corresponding to a maximum value of the reconnection rate. This maximal reconnection rate is a function of the magnetic Reynolds number given in an implicit form

$$\varepsilon = \frac{\pi}{4(A + \ln(\mathrm{Re}_m/\varepsilon))}, \tag{45}$$

where A is the constant $A = 3 - 2\ln(\tilde{\varepsilon}) - 3\ln(12/\pi) = -0.31$. Here Re_m is the Reynolds number determined for the global scale and the maximal resistivity $Re_m = 4\pi V_A L/(c^2 \eta_{\max})$. This result can be interpreted as follows. In the case of a large global Reynolds number, for fixed values of the maximum resistivity and the global scale L, the reconnection rate and the corresponding intensity of energy conversion reach their maxima when the diffusion region length scale and also the conductivity length scale are much smaller than L. This maximum value of the reconnection rate is a logarithmic function of the global Reynolds number which is similar to that estimated by Petschek. This fact contradicts to the usual electrotechnical intuition. For example, to get maximum heating from a rheostat (resistor), we need to switch on the whole length, to increase l_d, as opposed to the progress of reconnection. It is a fact that the energy release in the course of the reconnection process takes place not only in the form of Joule heating in the diffusion region and at the shock fronts, but also in the form of plasma acceleration.

By increasing the conductivity length scale and the corresponding diffusion region length scale, the reconnection rate decreases substantially, becoming more close to that of the Sweet–Parker regime.

We have to emphasize once more that the case of constant resistivity is not described by Eq. (44), because there is no clear scale of the diffusion region, no clear Petschek-type asymptotic behavior, and therefore, it cannot be matched with the Petschek solution.

The appearance of strongly localized resistivity is often the relevant case in space plasma applications, but for laboratory experiments, where the size of a device is relatively small, the Petschek regime can hardly be expected.

One of the main difficulties of the diffusive-like theories of reconnection such as the Sweet–Parker mechanism (Sweet, 1958,[5] Parker, 1963[14]), and the tearing instability (Galeev *et al.*, 1986[15]) is that the efficiency of the process turns out to be of the order of $Re_m^{-\alpha}$ where usually $0 < \alpha < 1$. For example, for the Sweet–Parker regime, $\alpha = 1/2$. In cosmic plasmas the magnetic Reynolds number is often very large because of the large scale, high velocity, and high conductivity. Hence, the efficiency of pure dissipative processes is rather poor. The Petschek mechanism of fast reconnection is much more effective due to the logarithmic dependence of the reconnection rate on scale (42). In the Petschek model, MHD waves play the dominant role and the logarithmic dependence is the contribution of the waves to the efficiency of the process.

In this paper, we studied reconnection for a strongly localized resistivity with a large ratio of the maximal and background resistivity (20). A crucial parameter for the reconnection rate is the diffusion region length which is obtained to be approximately equal to the length scale of the resistivity. An interesting question for future study is the dependence of the diffusion region length as well as the electric field on the amplitude of the resistivity variation.

ACKNOWLEDGMENTS

This work is supported by the INTAS-ESA project 99-01277. It is also supported in part by Grant Nos. 01-05-65070 and 01-05-64954 from the Russian Foundation of Basic Research and by the programme ''Intergeophysics'' from the Russian Ministry of Higher Education. Part of this work is supported by the ''Fonds zur Förderung der wissenschaftlichen Forschung,'' project P13804-TPH. This work is further supported by Grant No. 01-05-02003 from the Russian Foundation of Basic Research and by project I.4/2001 from ''Österreichischer Akademischer Austauschdienst.'' We acknowledge support by the Austrian Academy of Sciences, ''Verwaltungsstelle für Auslandsbeziehungen.''

APPENDIX: MATHEMATICAL DETAILS

So, we have to clarify the problem concerning the asymptotic behavior $B_y(x/l_d)\to 2\varepsilon' B_d$ when $x/l_d\to\infty$, estimate the integral, and to prove that the global Petschek solution tends to the local one if we take into account all necessary terms. Originally, Petschek[5] considered the reconnection problem using as a small parameter the reconnection rate ε. He obtained the solutions (11)–(16), taking into account only zero- and first-order terms in the inflow region, and zero-order terms in the outflow region. But there is the possibility to extend this solution with higher-order terms (Pudovkin and Semenov[16]). In order to do this we have to present each component of the MHD state vector U (inflow region), $\hat{U}$ (outflow region), S (shock front) as an asymptotic series with respect to the reconnection rate ε

$$U=U^{(0)}+\varepsilon U^{(1)}+\varepsilon^2 U^{(2)}+\cdots, \tag{A1}$$

$$\hat{U}=\hat{U}^{(0)}+\varepsilon \hat{U}^{(1)}+\varepsilon^2 \hat{U}^{(2)}+\cdots, \tag{A2}$$

$$S=S^{(0)}+\varepsilon S^{(1)}+\varepsilon^2 S^{(2)}+\cdots. \tag{A3}$$

The terms of the series (A1)–(A3) can be obtained step by step using the MHD equations (2)–(4) and the shock boundary conditions (5)–(9) according to the following scheme:

$$U^{(0)}\overset{1}{\Rightarrow}\hat{U}^{(0)}\overset{2}{\Rightarrow}S^{(0)}\overset{3}{\Rightarrow}U^{(1)}\overset{4}{\Rightarrow}\hat{U}^{(1)}\overset{5}{\Rightarrow}S^{(1)}\overset{6}{\Rightarrow}\cdots. \tag{A4}$$

Here $U^{(0)}$ is the initial vector, and each next term is determined via solving the reduced MHD system with boundary condition provided by the previous step.

For example, the original Petschek solutions (11)–(16) corresponds to the first three steps of this scheme. The first step is trivial, because no shock front is yet possible. In the next step, the outflow region solution of zero order allows to impose a boundary condition problem for the inflow region solution in first order, and so on.

Proceeding according to this scheme up to the step 5, we obtain the following extended Petschek solution. Inflow region

$$B_x=B_0-\frac{4\varepsilon}{\pi}B_0\ln\frac{L}{\sqrt{x^2+y^2}}, \tag{A5}$$

$$B_y=\frac{4\varepsilon}{\pi}B_0\arctan\frac{x}{y}, \tag{A6}$$

$$V_x=\frac{4\varepsilon}{\pi}V_0\arctan\frac{x}{y}, \tag{A7}$$

$$V_y=-V_0-\frac{4\varepsilon}{\pi}V_0\ln\frac{L}{\sqrt{x^2+y^2}}. \tag{A8}$$

Outflow region

$$B_x=\frac{4\varepsilon}{\pi}B_0\ln\frac{x+\hat{y}}{x-\hat{y}}, \tag{A9}$$

$$B_y=\varepsilon B_0-\frac{4\varepsilon^2}{\pi}B_0\ln\frac{x^2-\hat{y}^2}{4xL}, \tag{A10}$$

$$V_x=V_A+\frac{4V_0}{\pi}\ln\frac{x^2-\hat{y}^2}{4Lx}, \tag{A11}$$

$$V_y=\frac{4\varepsilon V_0}{\pi}\left(\ln\frac{x+\hat{y}}{x-\hat{y}}+\frac{\hat{y}}{x}\right), \tag{A12}$$

where $\hat{y}=y/\varepsilon$.

Shock front equation

$$y=\varepsilon x+\frac{4\varepsilon^2}{\pi}\left(2x\ln\frac{x}{L}+x\right). \tag{A13}$$

Finally it is possible to find the y-component of the magnetic field $B_y(x)$ at the shock which has been used in deriving the reconnection rate up to second order

$$B_y=2B_0\varepsilon\left(1-\frac{4\varepsilon}{\pi}\left(\ln\frac{x}{L}+3\right)\right). \tag{A14}$$

Using the extended Petschek solutions (A5)–(A14), we can prove now that the global solution tends to the local one at $x\sim l_d$. From Eqs. (39) and (41) it follows that

$$\varepsilon'=\varepsilon B_0^2\left(1+\frac{8\varepsilon}{\pi}\ln\frac{L}{l_d}\right). \tag{A15}$$

Let us check now that $B_y(x)\to 2\varepsilon' B_0'$ for $x\sim l_d$ at the inflow side of the shock. On one hand, we can expect that near the diffusion region

$$\begin{aligned}B_y'=2\varepsilon' B_0'&=2B_0\varepsilon\left(1+\frac{8\varepsilon}{\pi}\ln\frac{L}{l_d}\right)\left(1-\frac{4\varepsilon}{\pi}\ln\frac{L}{l_d}\right)\\&=2B_0\varepsilon\left(1+\frac{4\varepsilon}{\pi}\ln\frac{L}{l_d}\right).\end{aligned} \tag{A16}$$

On the other hand, for $x\sim l_d$, the global solution tends to

$$\begin{aligned}B_y&=2B_0\varepsilon\left(1-\frac{4\varepsilon}{\pi}\left(\ln\frac{x}{L}+3\right)\right)_{x=l_d}\\&=2B_0\varepsilon\left(1+\frac{4\varepsilon}{\pi}\ln\frac{L}{l_d}\right).\end{aligned} \tag{A17}$$

Therefore, $B_y(x)\to 2\varepsilon' B_0'$, if we take into account the next term in the ε expansion for B_y at the shock. This resolves the question concerning the asymptotic behavior $B_y(x/l_d)\to 2\varepsilon' B_d$ when $x/l_d\to\infty$.

Similarly it can be shown that the global Petschek solution tends to the local one at the distance $x\sim l_d$. This implies

that all components of **V**, **B** are matched automatically near the boundary with the convection zone if one of them (B_x in our case) has been adjusted properly.

Now we can estimate the integral used in Eq. (34)

$$\frac{1}{\pi}\int_{-L}^{L}\frac{(B_y(x',0)-B_y^P(x',0))}{x'}dx' = \frac{1}{\pi}\int_{-L}^{-l_d}+\frac{1}{\pi}\int_{-l_d}^{l_d}+\frac{1}{\pi}\int_{l_d}^{L}. \tag{A18}$$

The integral over the diffusion region $x\in(-l_d,l_d)$ is estimated as $O(\varepsilon)$ since $B_y(x,0)-B_y^P(x,0)$ is an odd function of x, and the integral converges in the usual sense rather than to be calculated as a principal value. The contribution from the intervals $(-L,-l_d)$ and (l_d,L) are estimated as $O(\varepsilon^2\ln(L/l_d))$ because as it follows from Eq. (A17), the difference $B_y(x,0)-B_y^P(x,0)\sim O(\varepsilon^2\ln(L/l_d))$. Taking into account the hierarchy of the small parameters (37) we conclude that the whole integral (A18) is estimated as $O(\varepsilon)$.

[1] E. W. Hones, Jr., *Magnetic Reconnection in Space and Laboratory Plasmas*, Geophysical Monograph 30 (American Geophysical Union, Washington, 1984).
[2] E. R. Priest, Rep. Prog. Phys. **48**, 955 (1985).
[3] E. N. Parker, J. Geophys. Res. **62**, 509 (1957).
[4] P. A. Sweet, *Electromagnetic Phenomena in Cosmic Physics*, edited by B. Lehnert (Cambridge University Press, Cambridge, 1958), p. 123.
[5] H. E. Petschek, Magnetic field annihilation, *NASA Spec. Publ.*, SP-50, 425 (National Aeronautics and Space Administration, Washington, DC, 1964).
[6] D. Biskamp, Phys. Fluids **29**, 1520 (1986).
[7] M. Scholer, J. Geophys. Res. **94**, 8805 (1989).
[8] H. Ji, M. Yamada, S. Hsu, R. Kulsrud, T. Carter, and S. Zaharia, Phys. Plasmas **6**, 1743 (1999).
[9] M. Ugai, Phys. Plasmas **6**, 1522 (1999).
[10] N. V. Erkaev, V. S. Semenov, and F. Jamitzky, Phys. Rev. Lett. **84**, 1455 (2000).
[11] V. M. Vasyliunas, Rev. Geophys. Space Phys. **13**, 303 (1975).
[12] L. D. Landau and E. M. Lifschitz, *Lehrbuch der Theoretischen Physik, Klassische Feldtheorie* (Akademie-Verlag, Berlin, 1984).
[13] D. A. Uzdensky and R. M. Kulsrud, Phys. Plasmas **7**, 4018 (2000).
[14] E. N. Parker, Astrophys. J., Suppl. Ser. **8**, 177 (1963).
[15] A. A. Galeev, M. M. Kuznetsova, and L. M. Zelenyi, Space Sci. Rev. **44**, 1 (1986).
[16] M. I. Pudovkin and V. S. Semenov, Space Sci. Rev. **41**, 1 (1985).